



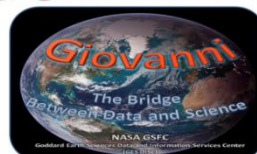
Blocking anticyclone over European Russia in the summer of 2010: interplay between atmospheric dynamics and composition

Sergei Sitnov ¹, Igor Mokhov ¹, Anthony Lupo ², and Alexander Timazhev ¹

¹ A. M. Obukhov Institute of Atmospheric Physics, Russian Academy of Sciences, Moscow, Russia

² Department of Soil, Environmental and Atmospheric Sciences, University of Missouri, Columbia, MO, USA

2014
Gregory G. Leptoukh



2nd Online Giovanni Workshop

Motivation

- Extreme hot weather in summer and extreme cold weather in winter are associated with the phenomena of atmospheric blockings (Lupo et al., 2012)
- In the Northern Hemisphere the maximum blocking activity is observed in the Euro-Atlantic sector (Weidenmann et al., 2002; Mokhov et al., 2014)
- Continental blocks are relatively more frequent in summer (Bariopedro et al., 2010)
- In summer the maximum blocking frequency in the Euro-Atlantic sector is observed approximately at 30°E, i.e. over eastern Europe and western Russia (Bariopedro et al., 2006).
- Under twenty-first century high emission scenario, CMIP5 models reveal in summer an eastward shift of blocking in a region close to the blocking that dominated the Russian summer of 2010 (Masato et al., 2013)

Aim

- Analysis of changes in atmospheric composition associated with unusually prolonged atmospheric blocking over European Russia in the summer of 2010

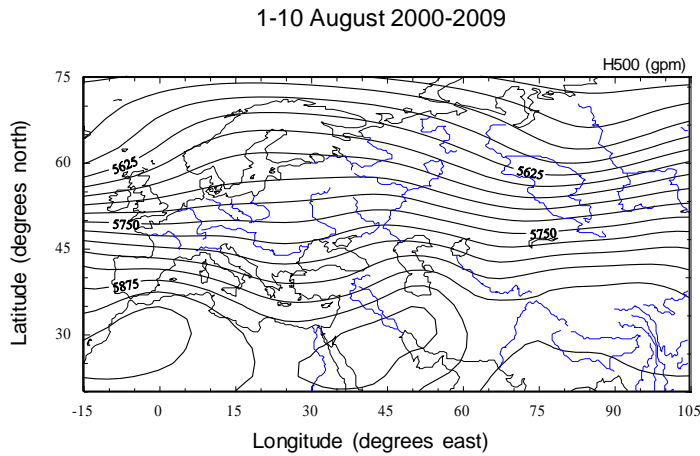
Data used

- Aerosol optical depth (AOD) at $\lambda=0.55 \mu\text{m}$, MODIS (Aqua and Terra), V5.1, L3 (Giovanni)
- Active fires, MODIS (Aqua and Terra), V2.4, L2, $p \geq 80\%$ (FIRMS)
- Cloud fraction (land), MODIS (Aqua and Terra), V5.1, L3 (Giovanni)
- Nitrogen dioxide (NO_2) tropospheric column, OMI (Aura), V3, L2G (Giovanni)
- Formaldehyde (HCHO) column amount, OMI (Aura), V3, L2G (Giovanni)
- Erythemal UV daily dose, OMI (Aura), V3, L3 (Giovanni)
- Ozone (O_3) volume mixing ratio, MLS (Aura), V3.3, L2 (Giovanni)
- Carbon monoxide (CO) total column, MOPITT, V4, L3 (Langley ASDC-data pool)
- Total column ozone, AIRS (Aqua), V5.2.2, L3 (Giovanni)
- Total column water vapor, AIRS (Aqua), V5.2.2, L3 (Giovanni)
- Water vapor (H_2O) mass mixing ratio at 150 hPa, AIRS (Aqua), V5.2.2, L3 (Giovanni)
- Methane (CH_4) volume mixing ratio at 160.5 hPa, AIRS (Aqua), V5.2.2, L3 (Giovanni)
- Tropopause height, AIRS (Aqua), V5.2.2, L3 (Giovanni)
- Tropopause temperature, AIRS (Aqua), V5.2.2, L3 (Giovanni)
- Meridional and zonal winds at 925, 700, 500, 200, 150, 70 hPa ($2.5^\circ \times 2.5^\circ$), NCEP/NCAR reanalysis
- Geopotential heights, ($2.5^\circ \times 2.5^\circ$), NCEP/NCAR reanalysis

Data sources

- Giovanni: <http://disc.sci.gsfc.nasa.gov/giovanni> (Acker and Leptoukh, 2007)
- FIRMS: <http://firefly.geog.umd.edu>
- Langley ASDC-data pool: <https://eosweb.larc.nasa.gov>
- NCEP/NCAR reanalysis: <http://www.esrl.noaa.gov>

Fig. 1a



The diagnostics of atmospheric blocking is commonly based on the analysis of the meridional gradient of 500-hPa geopotential height (H500).

The long-term distribution of H500 over Europe in the first ten days of August (Fig. 1a) is nearly zonal that reflects the dominance of westerly zonal transfer of air-masses in the region.

During blocking, the normal westerly flow pattern is disrupted. In the summer of 2010 the blocking episodes were observed over Europe in the period from June 22 to August 16. In the first ten days of August blocking anticyclone reached its maximum development. The results presented below, are provided mainly for this period.

The spatial distribution of H500 in the first ten days of August reveals the high over European Russia (ER) and two adjacent lows. This pattern is characteristic for omega block (Fig. 1b). H500 over ER reached 5910 gpm, that by 185 gpm exceeds the long-term average.

Atmospheric circulation in the free troposphere compelled air to move northward, eastward, and southward respectively in the western, northern, and eastern peripheries of the block area (Fig. 1c).

Characteristic for anticyclone conditions fair weather was observed in ER for a long time (Fig. 1e).

1-10 August 2010

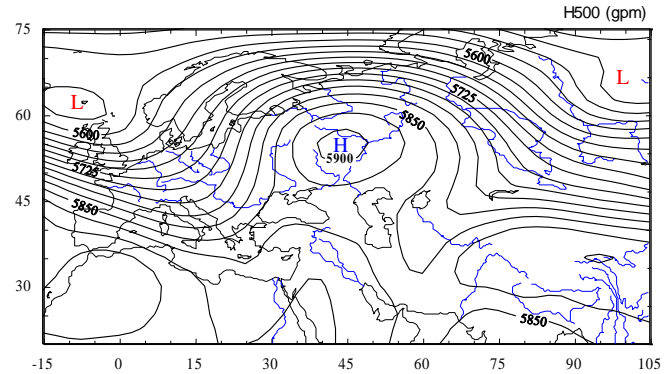


Fig. 1b

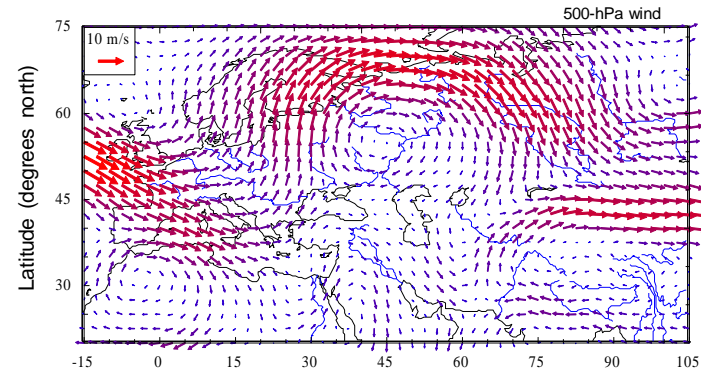


Fig. 1c

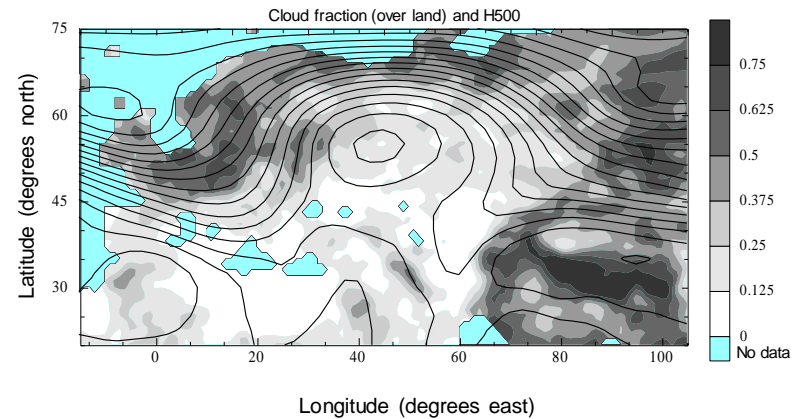


Fig. 1d

Wind 1-10 August 2010

Fig. 2a

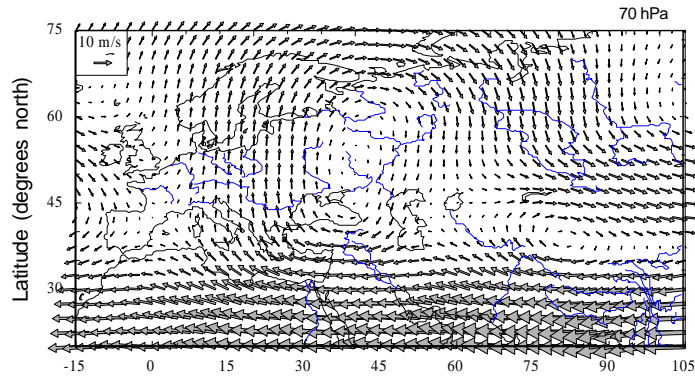


Fig. 2b

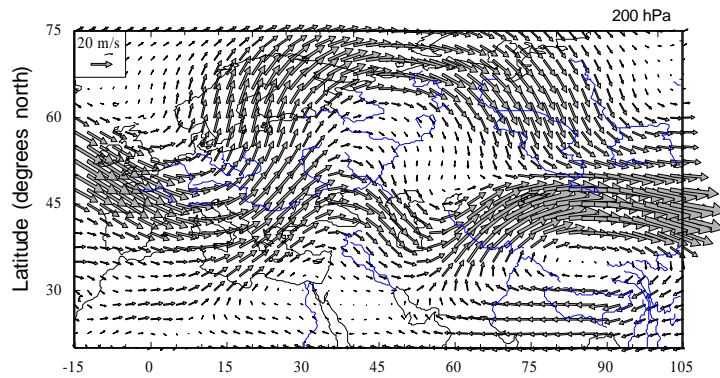
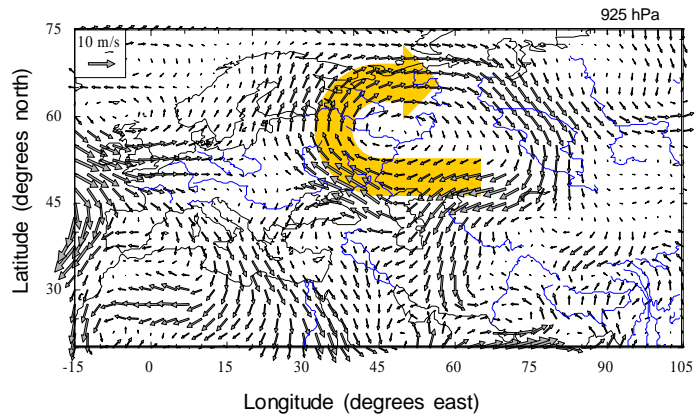


Fig. 2c



The blocking circulation manifested itself not only in the troposphere (Fig. 1b, Fig. 2c), but in the stratosphere (Fig. 2a).

In the tropopause region the atmospheric dynamics was characterized by intense wave disturbances (Fig. 2b) associated with quasi-stationary Rossby waves (Burkhardt and Lupo, 2005; Lupo et al., 2012).

The prolonged inflow of hot dry air originated from the deserts of Central Asia (the thick orange arrow), the intensive solar irradiation due to fair weather, and the lack of rainfalls led to the increase in surface temperature, to the soil drought and finely to the development of massive forest and peat bog fires in ER (Fig. 2d).

The fires caused the emission in the atmosphere of ER of the various products of biomass combustion.

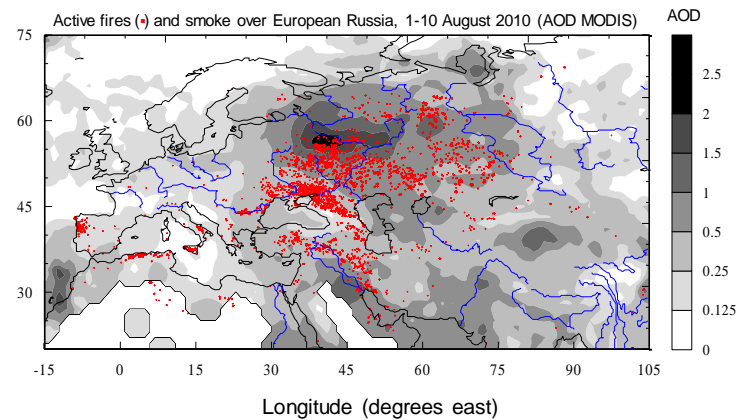


Fig. 2d

Biomass combustion products

1-10 August 2010

Fig. 3a

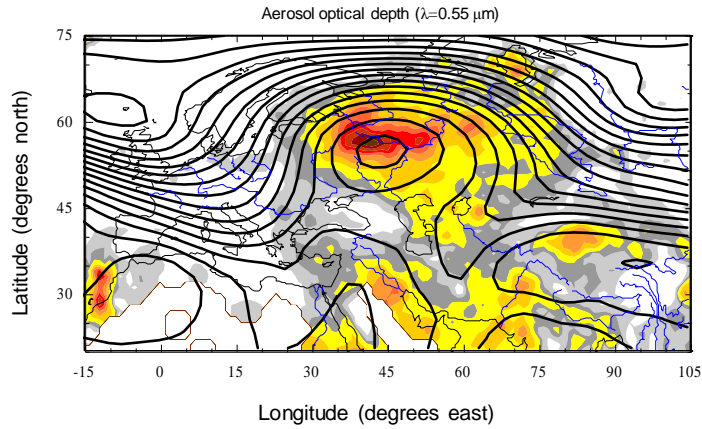
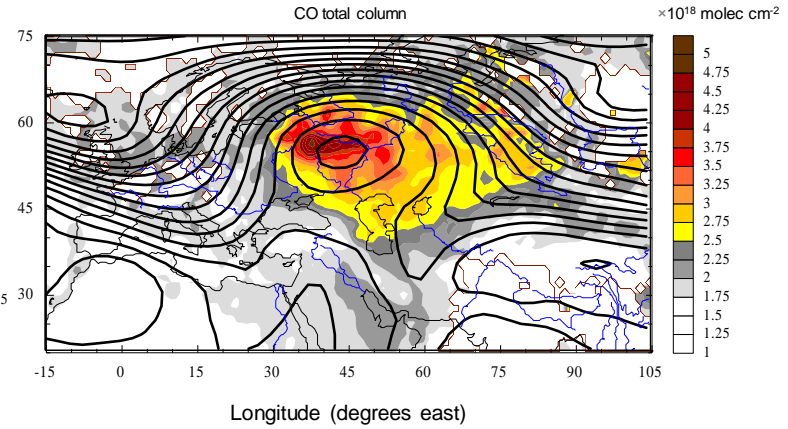


Fig. 3b



Aerosol optical depth (AOT) and carbon monoxide (CO) revealed the greatest increase during the wildfires (Fig. 3a, 3b). AOT over ER in this period mainly reflects the content of the particles of smoke in the air. In early August the daily mean AOT values (in the resolution of $1^\circ \times 1^\circ$) reached the value of about 4.9, that is more than 30 times higher than corresponding long-term mean AOT value. According to MOPITT data the daily mean CO total column (in the resolution $1^\circ \times 1^\circ$) in this period reached the value of 7.2 molec/cm^2 that 3.5 times exceeds corresponding long-term mean value (Sitnov, 2011a; Gorchakov et al. 2014)

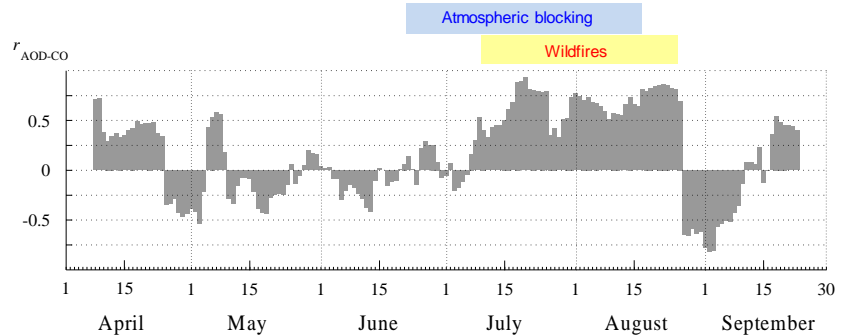


Fig. 3c

Fig. 3c shows the 15-day running correlation coefficients between daily values of AOT and CO averaged over the center of ER (52-59N, 29-45E). In the absence of wildfires the contents of aerosol particles and CO molecules in the air are controlled generally by different physical mechanisms. As a consequence the correlation coefficients between AOT and CO in these periods are characterized by different signs. During wildfires AOT positively correlated with CO, because in this period they both have one common source.

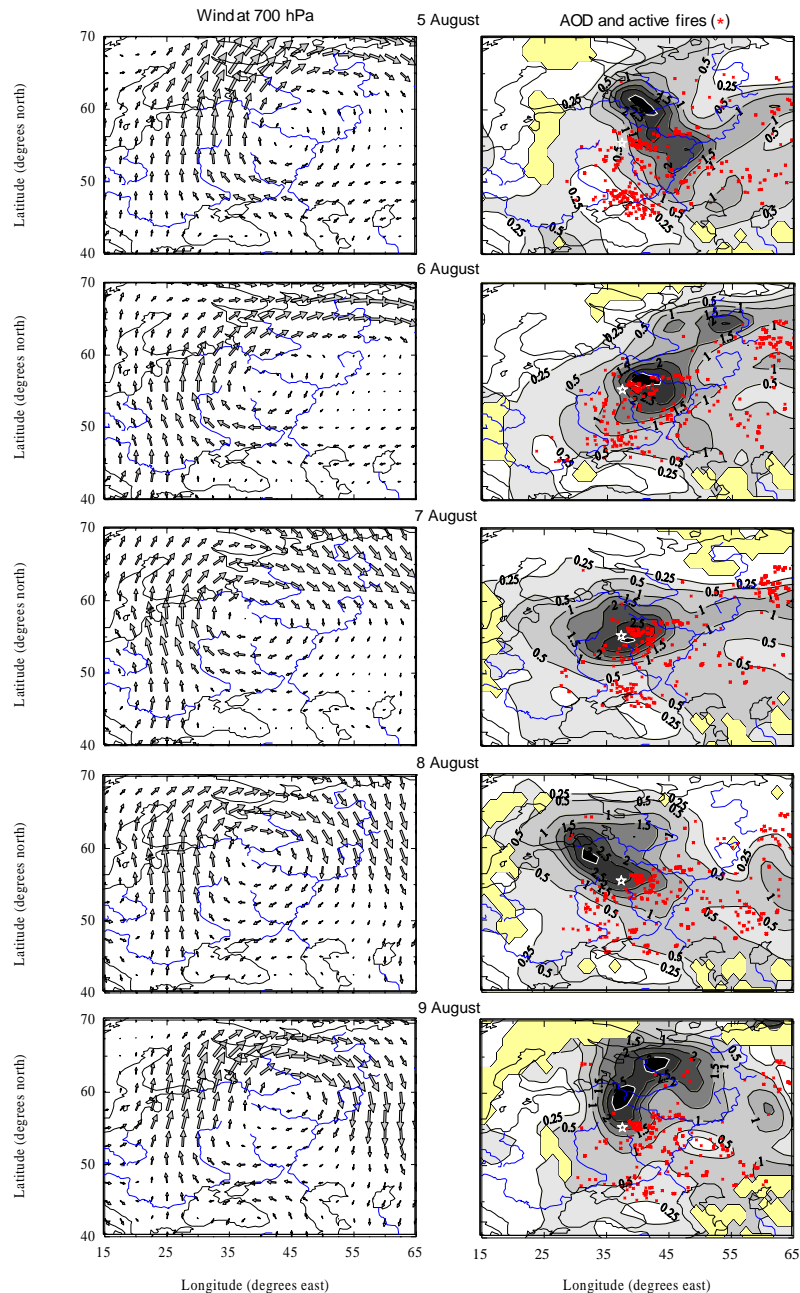


Fig. 4a

Fig. 4b

Spatio-temporal dynamics of the smoke plume

Day by day evolution of AOD during the extreme smoke period (5-9 August 2010) (Fig. 4b) to a great extent was conditioned by regional atmospheric dynamics associated with the block (Fig. 4a). Smoke has been involved in the anticyclonic circulation, characterized by weak winds in the center of the anticyclone and by strong winds on the periphery of it, spreading thus over the territory of ER. The vortex structure of the smoke distribution is clearly seen on August 9.

The obtained results testify that the maximum daily values of AOD over ER exceeded the daily mean AOD values observed in this period over Moscow by the factors of 1.5–3. The maximum AOD values over ER in the resolution of $1^\circ \times 1^\circ$ (4.86) was observed on August 7 at the distance 250 km south from Moscow. Tracing in space and time the position of the extremely dense smoke domain ($\tau_{0.55} > 3$) reveals that during the period from 5 to 9 August the region of extremely high AOD values completed a full anticyclonic rotation around Moscow (white asterisk) remaining at a distance of 200–650 km from the megacity.

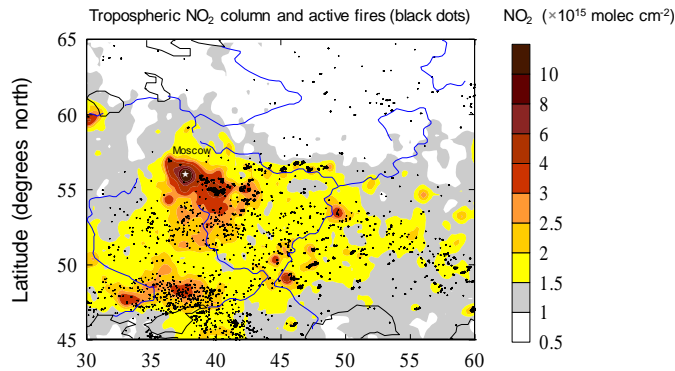
The migration of the plume of extreme smoke pollution on the megacity would have caused notable more severe consequences for the health of Moscow's inhabitants than those were observed.

Since the anticyclone center for a long time was located over the central cluster of wildfires, the Moscow's region was predisposed to prolonged smoky conditions, compared with the periphery of ER, where smoke could be rather strong, but short-lived.

Biomass combustion products (continued)

1-10 August 2010

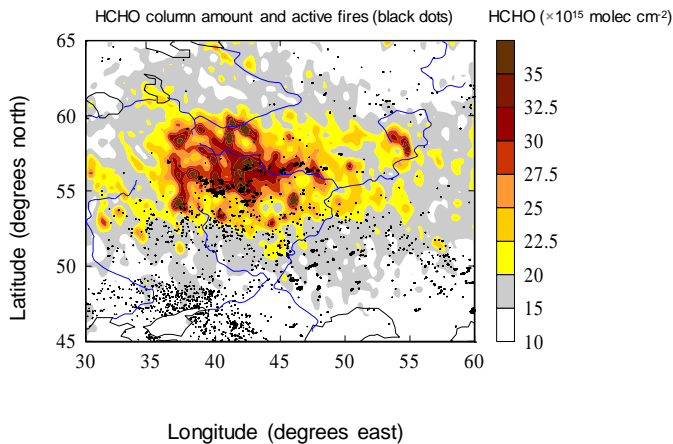
Fig. 5a



A greater number of short-lived products from combustion were concentrated near the clusters of fires (Fig. 5a, b) which were located in the center of ER (Sitnov, 2011b).

In the first ten days of August 10-day average HCHO atmospheric column over the territory restricted by the coordinates 54°-57°N and 38°-48°E has more than doubled in comparison with the long-term mean and reached the value of 28 molec/cm² (Fig. 5b).

Fig. 5b

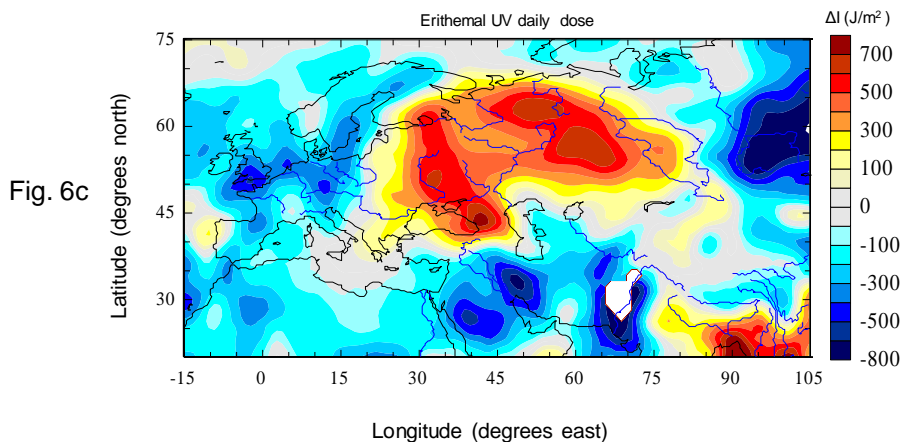
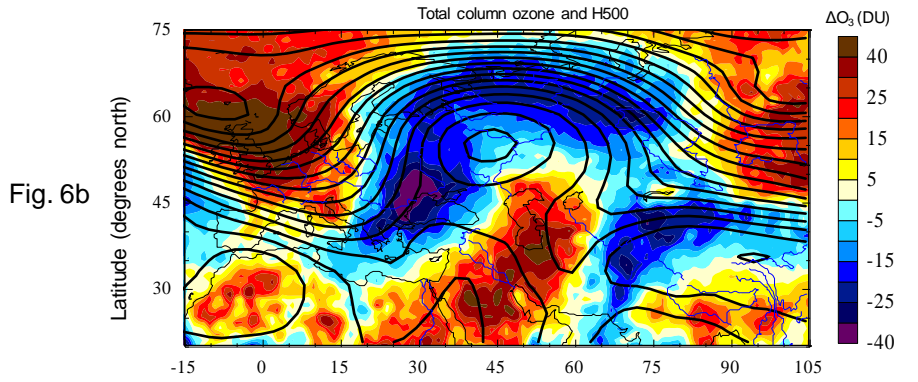
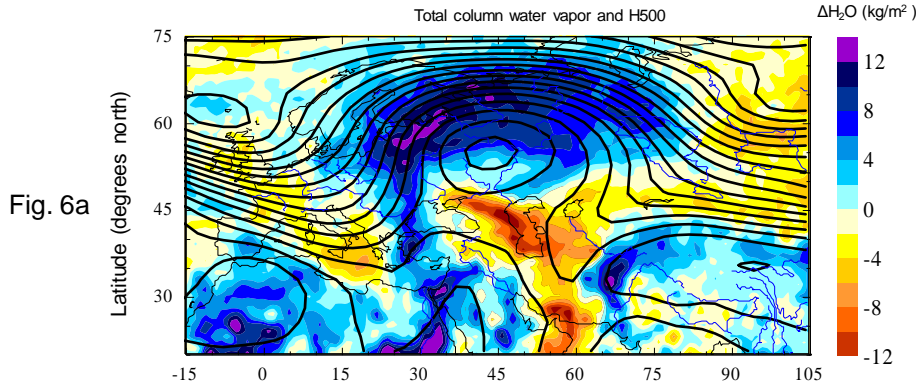


The increase in NO₂ was less noticeable (Fig. 5a). Tropospheric NO₂ content in early August over the territory specified above reached the value of 2.3 10¹⁵ molec/cm² that corresponds to 35% increase.

Characteristically, the NO₂ content over Moscow megalopolis substantially exceeded the content of NO₂ over the central cluster of fires, centered at 55°N, 40°E

Total column water vapor, ozone, and erythemal UV daily dose

1-10 August 2010



In addition to the increase of the contents of burning products, there were also changes in the regional atmospheric composition which were conditioned by the large-scale atmospheric dynamics.

Fig. 6a shows the anomaly of total water vapor content in the first ten days of August 2010. Hereinafter spatial anomalies (Δ) were calculated as the differences between the local mean values in the period 1-10 August 2010 and the corresponding long-term mean values in the periods 1-10 August 2003-2013 (with the exception of 2010). It is seen that the advection of moist Mediterranean and Atlantic air to the north of ER contributed to the formation of abnormal spatial distribution of total column water vapor with an excess of water vapor over the northern ER (70%) and its deficit over the southern part of the region (40%) (Sitnov et al., 2014; Sitnov and Mokhov, 2015).

The spatial distribution of total column ozone (TCO) anomalies has also been associated with anomalies of atmospheric circulation (Fig. 6b). An extensive region of negative TCO anomalies of total area more than 11 million km² in which TCO anomalies reached the value of -37 Dobson units (DU) (11%) was observed over the western and northern periphery of the anticyclone. Positive anomalies of TCO reaching the values of 60 DU (17%) were observed over the regions adjacent to the blocking area. In the middle and high latitudes the anticorrelation between spatial distributions of anomalies in total column water vapor and in total column ozone is noticed (Sitnov and Mokhov, 2015) that seems rather unexpected because almost all water vapor is concentrated in the lower troposphere, while the basic amount of ozone is in the stratosphere.

TCO regulates the intensity of biologically active solar UV radiation coming to the Earth's surface. As a consequence in the region of negative TCO anomalies the increased levels of UV radiation were observed (Fig. 6c). In early August 2010, over the territory restricted by the coordinates 50°-65°N and 30°-70°E the average daily dose of erythemal UV radiation reached 3000 J/m², which is 20% higher than the corresponding long-term value.

1-10 August 2010

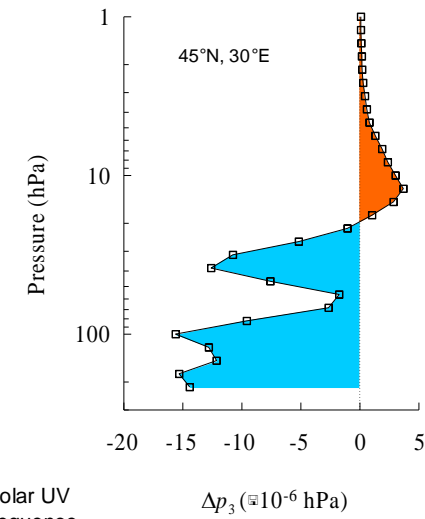


Fig. 6d

Tropopause region

1-10 August 2010

Wind at 200 hPa

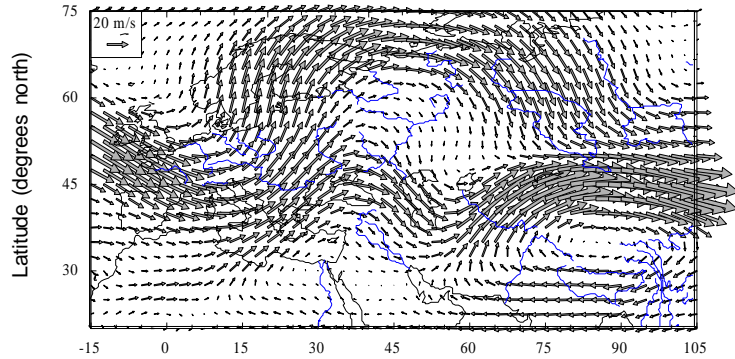


Fig. 7a

When comparing the distribution of average wind in the tropopause region (Fig. 7a) with TCO distribution (Fig 6b), it is seen that the negative anomaly in TCO in the block area can be associated with the transport of subtropical air masses with low TCO to the north in the sector 20°-40°E.

Tropopause height

ΔH (m)

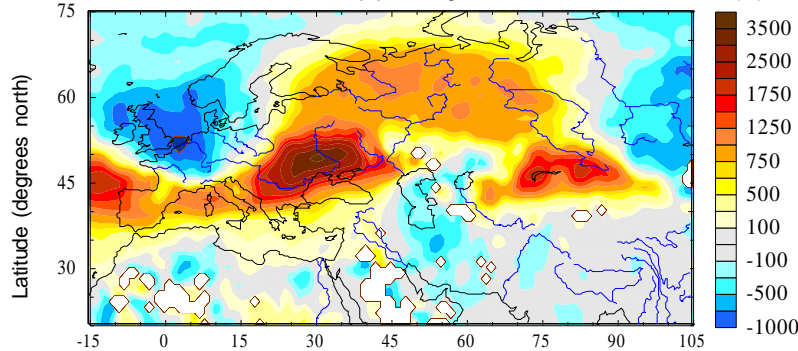


Fig. 7b

The spatial distributions of anomalies in tropopause height (Fig. 7b) and temperature (Fig. 7c) evidence that the decrease of TCO can be also associated with the tropopause rising in the block area. The local minimum of TCO centered at 45°N, 30°E is difficult to explain by isentropic ozone transport. Anticorrelation between ΔH and ΔT suggests a dynamic relationship between these tropopause characteristics, which is typical for vertical motions. Ascent of air in the upper troposphere and lower stratosphere is associated with adiabatic cooling of air and, as a consequence, with the increase in tropopause height and the decrease in tropopause temperature. The increase in tropopause height leads to the replacement of the lower stratospheric air with a relatively high ozone mixing ratio by the upper tropospheric air with a relatively low ozone mixing ratio, which results in TCO decrease.

Tropopause temperature

ΔT (°C)

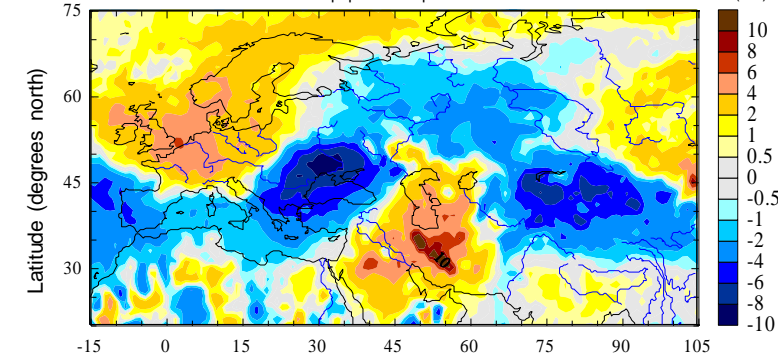


Fig. 7c

The variations in TCO reflect changes of ozone at different altitudes. Fig. 6d shows the anomalies of ozone partial pressure (Δp_3) in the first ten days of August 2010 in the region of strong reduction of TCO, centered at 45°N, 30°E (see Fig. 6b). It is seen that ozone decreased below 20 hPa (26.5 km) and increased above this level (Sitnov and Mokhov, 2015). The opposite changes of ozone in the lower and middle stratosphere is apparently due to opposite climatological meridional gradients of p_3 in the lower stratosphere (positive) and in the middle stratosphere (negative).

Longitude (degrees east)

Water vapor and methane in the mid-latitude lower stratosphere

1-10 August 2010

Wind at 150 hPa

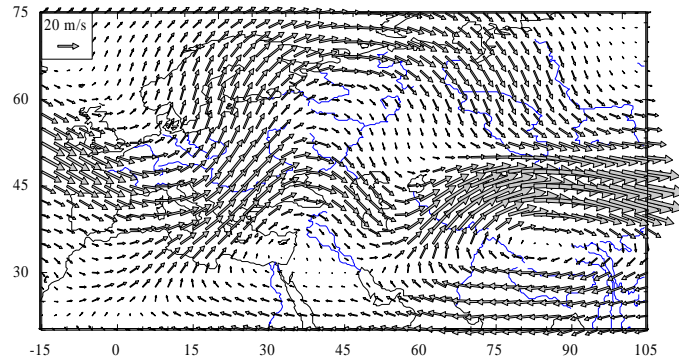


Fig. 8a

H₂O mass mixing ratio at 150 hPa

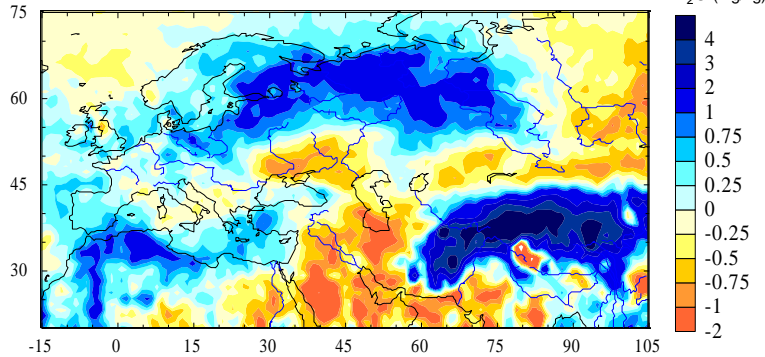


Fig. 8b

CH₄ volume mixing ratio at 160.5 hPa

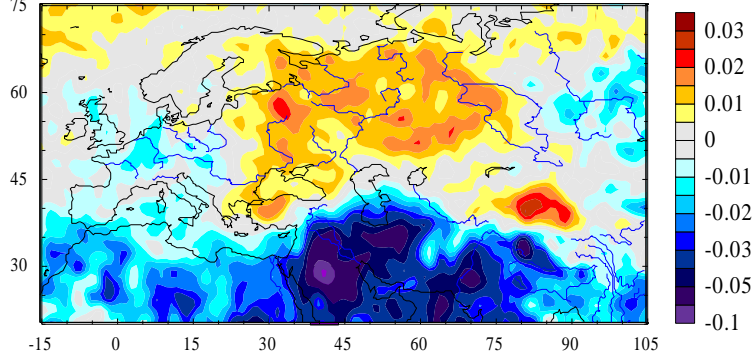


Fig. 8c

Longitude (degrees east)

As associated with the atmospheric dynamics, the decrease in TCO during atmospheric blocking in the summer of 2010 can be also attributed to the photochemical destruction of ozone in the lower stratosphere.

Fig. 8b and 8c show the anomalies of water vapor ($\Delta\text{H}_2\text{O}$) and methane (ΔCH_4) in the lower stratosphere. The spatial distribution of $\Delta\text{H}_2\text{O}$ and ΔCH_4 at these heights are also largely shaped by the dynamic factors (cf. Fig. 8b and Fig. 8c with Fig. 8a). Oxidation of H_2O (and CH_4) is a major source of hydroxyl radicals (OH) in the stratosphere, whose content modulates the intensity of catalytic cycle of ozone destruction.

Thus an increase in H_2O and CH_4 in the lower stratosphere should lead to a decrease in ozone concentration in this height region and as a consequence to a decrease in TCO.

Conclusion

- Changes in atmospheric composition during unusually prolonged atmospheric blocking over European Russia in the summer of 2010 were due to:
- emission of combustion products into the atmosphere from massive forest and peat bog fires
- advection of atmospheric constituents, whose climatological spatial distributions are characterized by zonality and perceptible meridional gradient
- changes in the height of the tropopause
- vertical motions

Literature

- *Acker J. G., Leptoukh G.* Online Analysis Enhances Use of NASA Earth Science Data. *Eos, Trans. AGU.* 2007. V. 88. No. 2. P. 14-17
- *Barriopedro D., Garcia-Herrera R., Lupo A.R., Hernandez E.* A climatology of Northern Hemisphere blocking. *Journal of Climate.* 2006. V. 19. P. 1042–1063.
- *Barriopedro D., Garcia-Herrera R., J. F. Gonzalez-Rouco J. F., R. M. Trigo R. M.* Application of blocking diagnosis methods to General Circulation Models. Part II: Model simulations. *Climate Dynamics.* 2010. V. 35. P. 1393–1409.
- *Burkhardt J. P., Lupo A. R.* The planetary and synoptic-scale interactions in a Southeast Pacific blocking episode using PV diagnostics. *Journal of Atmospheric Sciences.* 2005. V. 62. P. 1901-1916.
- *Gorchakov G. I., Sitnov S. A., Sviridenkov V. A., et al.* Satellite and ground-based monitoring of smoke in the atmosphere during the summer wildfires in European Russia in 2010 and Siberia in 2012. *International Journal of Remote Sensing.* 2014. V. 35. No. 15. P. 5698-5721.
- *Lupo A. R., Mokhov I. I., Akperov M. G., et al.* A dynamic analysis of the role of the planetary and synoptic scale in the summer of 2010 blocking episodes over the European part of Russia. *Advances in Meteorology.* 2012. V. 2012. Article ID 584257. 11 pages
- *Lupo A. R., Oglesby R. J., Mokhov I. I.* Climatological features of blocking anticyclones: a study of Northern Hemisphere CCM1 model blocking events in present-day and double CO₂ concentration atmospheres. *Climate Dynamics.* 2014. V. 122. P. 265-270.
- *Masato G., Hoskins B. J., Woolings T.* Winter and Summer Northern Hemisphere Blocking in CMIP5 Models. *Journal of Climate.* 2013. V. 26. P. 7044-7059.
- *Mokhov I. I., Timazhev A. V., Lupo A. R.* Changes in atmospheric blocking characteristics within Euro-Atlantic region and Northern Hemisphere as a whole in the 21st century from model simulations using RCP anthropogenic scenarios. *Global and Planetary Change.* 2014. V. 122. P. 265-270.
- *Sitnov S. A.* Aerosol optical thickness and total carbon monoxide content over European Russia territory in the 2010 summer period of mass fires: Interrelation between the variations in pollutants and meteorological parameters. *Izvestiya, Atmospheric and Oceanic Physics.* 2011. V. 47. No. 6. P. 714-7128.
- *Sitnov S. A.* Satellite monitoring of atmospheric gaseous species and optical characteristics of atmospheric aerosol over European part of Russia in April-September 2010. *Doklady Earth Sciences.* 2011. V. 437. Part 1. P. 368-373.
- *Sitnov S. A., Mokhov I. I., Lupo A. R.* Evolution of water vapor plume over Eastern Europe during summer 2010 atmospheric blocking. *Advances in Meteorology.* 2014 V. 2014. Article ID 253953. 11 pages.
- *Sitnov S. A., Mokhov I. I.* Ozone mini-hole formation under prolonged blocking anticyclone conditions in the atmosphere over European territory of Russia in the summer of 2010. *Doklady Earth Sciences.* 2015. V. 460. No. 1 (in press).
- *Weidenmann J. M., Lupo A. R., Mokhov I. I., Tikhonova E. A.* The climatology of blocking anticyclones for the Northern and Southern Hemispheres: Block intensity as a diagnostic. *Journal of Climate.* 2002. V. 15. P. 3459-3473.

Acknowledgements

- Most of data used in this presentation were obtained via the Giovanni online data system, developed and maintained by the NASA GES DISC
- We acknowledge the mission scientists and Principal Investigators who provided the data used in this presentation